On glucose diffusivity of tissue engineering membranes and scaffolds

Hazwani Suhaimi, Shuai Wang, Tom Thornton, Diganta Bhusan Das*

Department of Chemical Engineering, Loughborough University, Leicestershire LE11 3TU, UK

(*Corresponding author; Email: D.B.Das@lboro.ac.uk; Tel: 00441509222509; Fax: 00441509223923)

Abstract

There has been an increasing interest in the concept of growing artificial tissues in bioreactors which use numerous membranes and scaffolds to support the cellular processes such as cell growth and nutrient uptake. While these approaches are promising and may be considered to be successful in some circumstances, there is a general lack of quantitative information on the glucose (nutrient) diffusivity of these materials. In addressing this issue we have carried out a series of well-defined laboratory experiments to measure the glucose diffusion coefficient across a number of tissue engineering membranes and scaffolds saturated with water and cell culture medium (CCM). For this purpose, a diffusion cell was constructed and five different membranes and scaffolds with varying pore size and shapes were employed, which include cellulose nitrate membrane, polyvinylidene fluoride membrane, poly(L-lactide) scaffold, poly(caprolactone) scaffold and collagen scaffold. Pore size distribution, porosity and tortuosity of these materials were then determined and correlated to the glucose diffusivity values. As expected, we found that the diffusion coefficient increases with increasing pore size of the materials. These relationships are non-linear and may be non-monotonic in nature as they depend on a number of factors such as the basic building blocks of the materials which are non-periodic and heterogeneous in nature and vary within the same material, or from one material to another. We observed that glucose diffusivities in the materials saturated with CCM are significantly reduced at a given temperature which is contrary to what have been generally assumed in the previous studies on glucose transport processes. Therefore, a conclusion can be drawn that the presence of extra components and difference in fluid properties of CCM compared to water have a significant effect on the glucose diffusion coefficient in the tissue engineering membranes and scaffolds.

Keywords: Membrane; Scaffold; Glucose; Diffusion coefficient; Tortuosity

1. Introduction

The concept of growing cells outside the human body and their survival has been proven to work dated back almost a century ago when Wilhelm Roux, a German zoologist, had successfully cultured chick neural crest in warm saline water for over a period of few days (Hamburger, 1997). This is

supported by Alexis Carrel, a Nobel Prize winner in 1912, whose work showed that not only it is possible to grow tissues including connective and heart tissues *in vitro* but also maintain their characteristics for over a long period of time (Carrel, 1912). Tissue engineering has emerged now to be a valuable tool as a solution to overcome health problems such as tissue damage, degeneration and failure.

Engineered bone (Kimelman-Bleich et al., 2011; Grayson et al., 2010), cartilage (Schulz et al., 2008), tendon (Abousleiman et al., 2009; Omae et al., 2012) and blood vessel tissues (L'Heureux et al., 2007) have been successfully cultured both *in vitro* and *in vivo* (Kimelman-Bleich et al., 2011; Omae et al., 2012; L'Heureux et al., 2007). But studies have shown that culturing functional tissues *in vitro* is more complex than *in vivo* due to the need for a controlled environment during cell cultivation (Li et al., 2013). Hence, a bioreactor system is essential. To date, there have been several types of bioreactors designed to culture and grow 3D tissues, such as spinner flasks (Page et al., 2013), rotating vessels (Nishi et al., 2013; Chao and Das, 2015), perfusion systems (Baptista et al., 2013), magnetic force bioreactors (Bock et al., 2010), compression or strain bioreactors (Abousleiman et al., 2009; Wartella and Wayne, 2009), combined bioreactors which may couple perfusion with compression (Liu et al., 2012) such as rotating compression bioreactors (Wu et al., 2013) and, another perfusion bioreactor, namely, hollow fibre membrane bioreactors (Ye et al., 2006; Abdullah et al., 2009; Napoli et al., 2011, 2014; Chapman et al., 2012). Even though these bioreactors give hopes to tissue engineering approaches, they may not be able to prolong the cell culture environments (Li et al., 2013). One of the reasons for this is limited nutrient diffusion through scaffolding matrix and membrane. To achieve the desired rate of mass transfer and allow the development of novel membranes and scaffold, a good understanding of the quantitative relationship between their properties and nutrient transport behaviour is essential (Chao and Das, 2015). A good understanding of the mass transfer behaviour in these materials is also necessary as these materials may be used to calibrate and develop biosensors, e.g., for monitoring glucose level (Boss et al., 2012; Wang et al., 2013).

One of the important components of most tissue engineering bioreactors is the scaffold/membrane matrix which acts as a support for cells to grow into new tissues before being implanted into the host tissue. Some of the general characteristics of the support materials are that they must be porous for ease of nutrient diffusion and waste product removal (Florczyk et al., 2013; Guan et al., 2013; Deans et al., 2012), biocompatible (Stamatialis et al., 2008), the material must possess comparable mechanical properties to that of *in vivo* tissues (Karageorgiou and Kaplan, 2005; Karande et al., 2004), allow cell seeding, and others. Some examples of these support materials for tissue engineering purposes are summarised in Table 1.

1 Table 1. Some examples of commonly used support porous materials and their characteristics

Material	**Fabrication technique**	**Pore size (μm)**	**Porosity (%)**	**Reference**
Poly(lactic-co-glycolic acid)(PLGA) scaffold	Fiber knitting	NA	NA	Ouyang et al. (2003); Sequeira et al. (2012)
Poly(caprolactone) (PCL) scaffold	Salt leaching and thermal induced phase separation	NA	93.6 ± 0.6	Zhang et al. (2013)
Hydroxyapatite (HA) scaffold	Imaging techniques and stereo lithography	250	40	Chu et al. (2002); Kim et al. (2007)
Poly(L-lactide)/β-tricalcium phosphate (PLLA/β-TCP) scaffold	Solvent self-proliferating/model compressing/particulate leaching	100-250	57	Xiong et al. (2002); Kang et al. (2009)
Collagen-glycosaminoglycan (GAG) scaffold	Lyophilisation technique	96	99.5	O'Brien et al. (2005); Keogh et al. (2010)
Poly(lactic-co-glycolic acid)(PLGA) membrane	Dry/wet- and wet-spinning	0.2-1.0	NA	Ellis and Chaudhuri (2006)
Poly(lactic-co-glycolic acid)(PLGA)/polyvinyl alcohol (PVA) membrane	Wet-spinning	0.54 ± 0.11 (PLGA) 0.67 ± 0.15 (1.25 % PVA-PLGA)	46 67	Meneghello et al. (2009)

		0.89 ± 0.16 µm (2.5% PVA-PLGA)	76	
		1.1 ± 0.1 µm (5 % PVA-	77	
Poly (lactide-co-glycolide)(P_{DL}LGA) membrane	Wet-spinning phase-inversion	0.16 ± 0.006	NA	Morgan et al. (2007)
Nanoporous polyethylene membrane	Stereolithography using a biocompatible medical-grade resin (proform)	0.01649	28.9 ± 4.93	Boss et al. (2012); Boss et al. (2011)
Polypropylene microporous membrane	Melt-extrusion/cold-stretch	0.10	45-50	Yu et al. (2008)
Titania nanotubular membrane	NA	0.125	60-70	Paulose et al. (2008)

Tissue growth and survival are undoubtedly complex, involving an immense variety of processes from intracellular transduction pathways to tissue-level mechanics (O'Dea et al., 2013). Cell differentiation, survival and proliferation of tissue-engineered constructs are highly dependent on the availability of nutrients. Therefore, the diffusion as well as the distribution and availability of the relevant solutes, e.g., nutrients, must be fully grasped as they are important for tissue formation, growth and survival (Liu et al., 2013). Glucose and oxygen are critical molecules in these regards as shown in both experimental and modelling studies (e.g., Mauck et al., 2003a; Ye et al., 2006). In contrast to oxygen which has been extensively studied over the years (Malda et al., 2004a, 2004b; Kellner et al., 2002; Guaccio et al., 2008; Ellis et al., 2001), there is limited knowledge available on the diffusion coefficients of other nutrients or metabolites especially glucose and lactic acid in porous membrane and scaffold within cell culture media (CCM) (Liu et al., 2013). Most diffusion coefficient data are for cases where these materials are saturated with water at ambient conditions. However, the cell/tissue culture experiments are typically conducted at 37-38^{o}C and the materials are imbibed with cell culture medium (CCM).

The diffusivities of glucose in aqueous solutions were measured some sixty years ago (Longsworth, 1952). More extensive measurements of glucose diffusion coefficients in different fluid and porous media have been studied as well, such as water (Dionne et al., 1996), poly-ether-sulphone and poly-sulphone (Curcio et al., 2005), polyvinyl alcohol (Phanthong and Somasundrum, 2003), calcium alginate (Chai et al., 2004), collagen gel (Shaw and Schy, 1981), agarose gel (Weng et al., 2005) and hemodialysis films and hollow fibers for blood purification processes (Klein et al., 1977). However, there is little or no published information that discuss specifically the glucose diffusivity across membranes or scaffolds that are used for cell/tissue engineering. Lactic acid is beyond the scope of this study and will not be covered here.

While a number of techniques have been studied and developed to study the diffusion of small molecules such as light scattering (Bica et al., 2001), nuclear magnetic resonance microscopy (NMR) (Kwak and Lafleur, 2003; George et al., 2004), fluorescence spectroscopy (Ye et al., 2003; McCain et al., 2004), fourier transform infrared microscopy (FTIR) (Sahlin and Peppas, 1996; Peppas and Wright, 1996), electrochemical techniques (Zhang et al., 2002; Cleary et al., 2003) and fluorescence recovery after photobleaching (FRAP) (Pluen et al., 1999), these often require sophisticated and indirect methods for the concentration measurements of the molecule diffusing across the membrane. These may not allow the diffusion process to be monitored continuously (Lu et al., 2013). Furthermore, the suitability of these techniques to study the materials investigated in the present study may not match with the materials' properties. For instance, the light transmission from and to the solute molecules in the gel-like scaffolds to capture its speed is not possible for used in the present study due to the

membranes/scaffolds investigated are generally not transparent. We propose in this study the use of a simple diffusion cell that is easy to use and allows us to monitor the diffusion process continuously over time.

The interest in the determination of diffusion coefficients in membranes particularly in chemical and biotechnological applications can be found in many applications of membranes, e.g., water treatments, drug delivery and tissue engineering (Choi et al., 2013; Bai et al., 2012; Jeon et al., 2012; Parizek et al., 2012; Peter et al., 2010). Despite a number of literature works, it does seem that the mass transfer behaviour in terms of dependence of diffusion on membrane morphology is still not fully understood (Wang and Ma, 2012). Molecular diffusion is dependent on the membrane morphology and the fluid that saturates it may have an effect on the diffusivity values (Cussler, 2009). Diffusional boundary layers that are created at the porous material-liquid interfaces may offer different resistances to diffusion as the fluid and materials change (Chan et al., 2012). The temperature of the system also plays important roles in determining the molecular diffusion. For example, the temperature affects both the solubility and diffusion coefficient of a molecule in a fluid and the porous material (Chen et al., 2013). The temperature also impacts the interactions among the multi-components that make up the fluid (e.g., a cell culture media) which may affect the diffusion coefficient of the molecule particularly if the molecular size is big (Abdullah and Das, 2007). What we obtain for the measurements of the diffusion coefficient of a molecule is therefore a lumped effect from a number of inter-related phenomena.

It is therefore the purpose of our study to quantify the relationship between diffusion coefficient and membrane morphology by engaging typical membrane and scaffold materials for tissue engineering in diffusion experiments and relating the diffusivity values to the quantitative information of the pore morphology of the materials. We acknowledge that some papers have discussed the dependence of the diffusion coefficient on temperature, for example, that by Yui et al. (2013) which discusses the change in diffusion coefficient of some solutes in water as temperature changes. Cai et al. (2012) reported the diffusion of glucose in membranes at 20°C and 37°C in deionized water and in NaCl solution. Umecky et al. (2013) also reported the influence of temperature on the values of the diffusion coefficient of amino acids in water. However, none of these papers really relate to the specific tissue engineering membranes, fluids (i.e., cell culture media) or combination of these two as they are normally used in tissue engineering.

In this study, we have adopted a two-compartment diffusion cell technique to investigate the glucose transport properties of typical tissue engineering membranes and scaffolds within CCM and water. This includes the relationship between the morphology of membranes and scaffolds and its effect on

glucose diffusivities. In addition, tortuosity and porosity as well as the diffusion coefficient of glucose in free media have been determined.

Please note that although the materials chosen for this study are designed for tissue engineering purposes, they are not seeded with any biological cells during our experiments. This is because this work is aimed at quantifying simple passive diffusion of glucose through the materials. As mentioned earlier, the diffusivity values are needed for a number of practical scenarios, e.g., modelling of mass transport in tissue engineering bioreactors, choosing the materials for tissue engineering bioreactors and biosensors, and any others. If indeed the membranes and scaffolds are seeded with biological cells (e.g., stem or epithelial cells; adherent or suspended cells), the mass transfer rate may be different due to their presence. The effective passive diffusion in this case may be different depending on a number of factors, e.g., density of cells in the materials, glucose uptake rate by the cells and any other factors. We consider this to be a 'derived' property and not discussed in this paper.

2. Materials and methods

2.1. Membranes

Two types of membranes were used in this study: cellulose nitrate (CN) and polyvinylidene fluoride (PVDF). The CN and PVDF membranes were purchased from Fisher Scientific UK Ltd (Loughborough, UK) and Millipore UK Ltd (Watford, UK), respectively. Table 2 shows the main characteristics of these membranes. Prior to conducting all experiments, the membranes were soaked in deionised water for a day in order to remove any remaining preservative on the membrane surface. We define that water fully imbibes into the membrane during this time period and, that there is no significant swelling and, hence, changes in the pore morphology of the membrane after this period. Table 3 shows the thicknesses of these membranes as measured using a surface profiling (non-contact mode) instrument (Talysurf CLI 2000, Taylor Hobson Ltd, Leicester, UK). The differences between the thicknesses at different time intervals are defined as due to the swelling of the membrane because of imbibition. The measurements were only done for water. As evident from the table, there is no significant change in the thickness of the membrane and, hence, swelling.

2.2. Scaffolds

Poly(caprolactone) (PCL), poly(L-lactide) (PLLA) and collagen scaffolds were used in this study. PCL was purchased from the Electrospinning Company Ltd (Didcot, UK) while PLLA was a kind gift from the same company. Collagen was purchased from Matricel GmbH (Herzogenrath, Germany). Table 2 shows the main characteristics of these scaffold materials. The appendix shows fibre density of the PCL and PLLA scaffolds as supplied by the manufacturer. Before their use, all scaffolds were treated as

follows. PCL was treated with 15% ethanol (Fisher Scientific UK Ltd, Loughborough, UK) for 30 min to aid in wetting the material and to remove any trapped air, before being soaked and washed with deionised water, replacing the water twice in 30 min in order to remove any trace of ethanol. The same treatment was applied to PLLA except that a 70% ethanol solution (Fisher Scientific UK Ltd, Loughborough, UK) was used. Collagen scaffold was pre-soaked in deionised water for 30 min before used in experiments. A different treatment was used in this case as the collagen scaffold is hydrophilic while both PCL and PLLA are hydrophobic in nature. Similar to the membranes, we define that there is no significant swelling and, hence, changes in the pore morphology of the scaffold after this period. Table 3 shows the thicknesses of these scaffold materials. Similar to the membranes, it is deduced that there is no significant swelling based on the results depicted in the table.

2.3. Other materials

The cell culture medium (CCM) used was Dulbecco's Modified Eagle Medium (DMEM) (Life Technologies Ltd, Paisley, UK). The glucose was of analytical grade powder D-glucose-anhydrous (Fisher Scientific UK Ltd, Loughborough, UK) of molecular weight 180.16 g/mol.

Table 2. Summary of the commercial membrane and scaffold properties

Material		Thickness (µm) based on Manufacturers' information	Manufacturers' pore size (µm)	Min pore size (µm)	Mean pore size (µm)	Max pore size (µm)	Source
Membrane	PVDF	125	0.1	0.08	0.32 ± 0.29	1.65	Merck Millipore (Watford, UK)
	CN	122.5	0.45	0.21	0.6 ± 0.30	2.09	Whatman International Ltd (Maidstone, UK)
Scaffold	PLLA	50	12-18	4.04	13.67 ± 4.25	25.87	The Electrospinning Company Ltd (Didcot, UK)
	PCL	50	20-30	5.8	21.69 ± 6.85	44.84	The Electrospinning Company Ltd (Didcot, UK)
	Collagen	1500	80	12.55	75.15 ± 5.21	175.18	Matricel GmbH (Herzogenrath, Germany)

Table 3. Material thicknesses as measured a surface profiling instrument (Talysurf CLI 2000, Taylor Hobson Ltd, Leicester, UK), and their respective swelling percentage. Please note that the average thicknesses we have measured vary slightly from the values of average thickness that the manufactures provide for the same samples (Table 2).

Material	Average thickness of dry sample (1) (μm)	Average thickness of wet sample after soaking in water for 24 hours (2), which represent the samples at the beginning of diffusion experiment (μm)	Average thickness of wet sample after soaking in water for 48 hours (3), which represent the samples at the end of diffusion experiments (μm)	Swelling between dry sample (1) and wet sample (2) (%)	Swelling between wet sample (2) and wet sample (3) (%)
PVDF membrane	98.38	98.61	101.23	0.23	2.66
CN membrane	124.22	125.54	129.79	1.06	3.39
PLLA scaffold	32.04	33.58	34.11	4.81	1.58
PCL scaffold	37.79	38.85	40.89	2.80	5.25
Collagen scaffold	1659.37	1699.9	1715.3	2.44	0.91

2.4. Determination of pore size distribution of the membrane and scaffold materials

Measurement of pore size is done manually using the software ImageJ (Wayne Rasband, National Institute of Mental Health). The analysis of the pore size distribution of the sample materials also used scanning electron microscopy (SEM) images where it enables visual images of membrane/scaffold's morphology and can be used directly in ImageJ software. Although these images refer to the surface morphology of the membranes and scaffolds investigated, they represent the sample morphology well as the samples have a fairly homogeneous (narrow range) of pore size distribution. The SEM images were uploaded on to the software and lines were drawn for every pore after setting the scale to track the measurements. The minimum, maximum and average of pore size are shown in Table 2. On the other hand, the pore size distributions for the selected materials are shown in Figure 3.

2.5. Evaluation of the porosity (ϵ) and tortuosity (τ) of the membrane and scaffold materials

Besides the pore size distribution, the porosity values of the materials were determined as they effect the solute diffusion through the materials. The porosity values depend on the size and distributions of the pores in the materials. Further, they are required to find out the tortuosity of each membrane/scaffold material in this study.

Porosity is defined as the ratio of voids volume to total volume:

$$\epsilon = 1 - \frac{V_m}{V_t} \quad (1)$$

Where, V_m is solid volume and V_t is total volume of sample.

Porosity can be determined either using indirect or direct approaches. Apparent densities estimation, pycnometric methods and mercury porosimetry are direct approaches while computerised analysis of scanning electron microscopy images and air-liquid displacement techniques are indirect approaches (Palacio et al., 1999). In this study, we opted for a direct approach, which is a pycnometric method. By measuring the masses and fitting the experimental data into the equation below, porosity is evaluated.

$$\varepsilon = 1 - \frac{m_1 + m_2 - m_3}{V_t \rho_w} \quad (2)$$

where m_1 is the mass of dry sample, m_2 is the mass of pycnometer levelled with water, m_3 is the mass of pycnometer levelled with water together with sample contained inside and ρ_w is the water density which is 0.9970 g/cm^3 at room temperature.

The dry membranes and scaffolds were each weighed separately before soaking them wet in the pycnometer. Assuming the porous materials were soaked completely and effectively in water, the masses of these wet samples were measured together with the water-levelled pycnometer, giving m_3. The experimental data were then fitted into Eq. (2) above giving porosity of the materials investigated.

Tortuosity, on the other hand, considers the increase in distance of a diffusing molecule due to pore bending and curves. Tortuous channels hinder the movement of molecules which gives resistance to mass transfer. This hindrance is included and defined by the tortuosity factor which takes into account the fluid transport system as well as the pore connectivity. A relatively straight channel gives a tortuosity value of unity while porous materials give a tortuosity value greater than unity, but typically between 2 and 3 (Martin, 1993).

Nuclear magnetic resonance (NMR) based measurements, mercury intrusion porosimetry, image analysis (Wu et al., 2006) and determination of the ratio of diffusion coefficient in free media to the diffusion coefficient in the porous network (Barrande et al., 2007) are some example methods used to evaluate the tortuosity. The latter is used in this study where the effective diffusion coefficient (D_e) is

derived from diffusivity measurements with the diffusion cell; porosity (ϵ) is derived from the aforementioned method and the diffusion coefficient in free media (D) is calculated from Stokes-Einstein equation described below. Hence, tortuosity (τ) is derived from the following relationship:

$$D_e = D\frac{\epsilon}{\tau} \quad (3)$$

It must be noted that different types of diffusivities are used in the above equation where D_e leads to transport diffusivity by fitting experimental measurements into Eq. (6) while D represent self-diffusivities calculated Stokes-Einstein equation (Eq. (9)).

2.6. Measurement of glucose diffusion coefficient

2.6.1. Diffusion cell for measurement of glucose diffusion coefficient

Two rectangular diffusion cells, which are similar to those described by Chenu and Roberson (1996), were made to measure the diffusion coefficient of glucose across the membranes and scaffolds in both CCM and water. Both cells consisted of two acrylic chambers with identical volumes. The chambers were called donor and receptor phase, respectively. A larger cell was used to determine the diffusion of glucose across the membranes and scaffolds in water while the smaller cell was used with CCM to help reduce the amount of CCM consumed per experiment. The diffusion cells were assembled by tightly screwing the half chambers into the rubber gaskets, with the membrane/scaffold fixed in between (Figure 1). The rubber gaskets were embodied to prevent leakage between the half chambers.

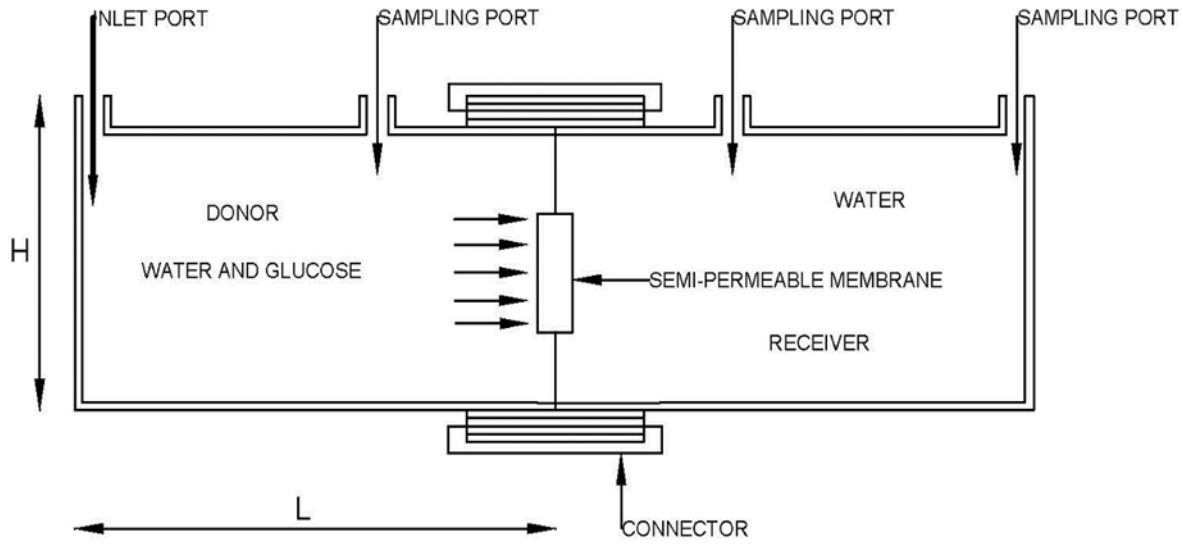

Figure 1. Schematic drawing of a diffusion cell

The larger cell has a volume of 207.5 ml per chamber with an internal geometry of length 100 mm x height 45 mm x width 50 mm. The smaller cell has a volume of 41 ml per chamber with an internal geometry of length 20 mm x height 45 mm x width 45 mm. Each half chamber was filled with either CCM or water. The donor phase also contained glucose solution. The glucose powder was pre-mixed in a beaker with either CCM or water prior to the start of the experiment. Both solutions of pure CCM/water (receptor phase) and glucose mixed with CCM/water (donor phase) were allowed to equilibrate at either 27 or 37°C in the heated water bath for 60 min before the apparatus was assembled. The whole apparatus was placed in a thermostated water bath at either 27 or 37 ± 1°C.

The corresponding diffusion coefficients were calculated according to Fick's first law. Fick's first law describes the diffusion of small uncharged molecules well. It is given by (e.g., Crank, 1975)

$$J = -D\frac{\partial C}{\partial z} \quad (4)$$

where J is the mass flux describing the mass transfer through an area per unit time, D is the diffusion coefficient of the solute molecule; C is the concentration of the diffusing solute molecule while z is the diffusion length. Obstruction effects as a result from diffusion across membranes and scaffolds must be considered with certain porosity and partition coefficient. These properties are included in the effective diffusion coefficient of the material (Gutenwik et al., 2004) defined by

$$J = -D_e\frac{\partial C}{\partial z} \quad (5)$$

Assuming that there was no change in volume, Eq. (5) was transformed into Eq. (6) and that the glucose diffusion across membranes and scaffolds in CCM was calculated as given below:

$$V_d\frac{\partial C_d}{\partial t} = -D_e A\frac{C_d - C_r}{l} \quad (6)$$

where l was the membrane/scaffold thickness, A the membrane/scaffold area, D_e the effective diffusion coefficient of the material and V_d the donor volume. By measuring the concentration in both chambers at different times, a diffusion coefficient was calculated by fitting Eq. (6) to the experimental data.

2.6.2. Measurements of glucose diffusion coefficients of the samples saturated in water

A UV spectrophotometer (UV Mini 1240, Shimadzu, Japan) was used to monitor the change in glucose concentration over time. Each chamber (Figure 1) was filled with 207.5 ml of deionized water as this is the amount that is required to fill the chamber completely. The donor phase also contained 2 mg/ml of glucose solution. Samples of 2.5 ml were taken using a plastic syringe from both the donor and receptor phase at intervals of 1 h until equilibrium was established. The samples were placed in a glass

cuvette and analysed by the UV spectrophotometer at a wavelength of 190 nm. Immediately after being analysed, the samples were poured back into the donor and receptor phase, respectively, to keep the volume constant. All experiments were conducted in duplicate.

2.6.3. Glucose monitoring system for diffusion in the materials saturated in CCM

An issue was encountered while investigating the diffusion of glucose in CCM. The photometric elusion curve showed significant noise at around 190 nm suggesting that the presence of other molecules in CCM might interfere and obscure the concentration measurements. To resolve this issue, a glucose analyser was used instead. To resolve this issues and to measure the diffusion of glucose in CCM, an YSI glucose analyser (YSI 2300 STAT PLUS, YSI UK Ltd, Hampshire, UK) was used. The outstanding performance of YSI glucose analyser has been known for more than two decades (Lindh et al., 1982; Clarke et al., 1987; Burrin and Alberti, 1990). It has been well accepted as a device for measuring glucose concentration due to its ease of use, quick analysing time (1 min) and small sample size (25 µl). This instrument is based on enzymatic reaction. The system consists of two membrane layers, an enzyme layer and a platinum electrode. The first layer which houses porous polycarbonate minimises the glucose diffusion into the enzyme layer to avoid the reaction from becoming enzyme-limited while the third layer which contains cellulose acetate only allows small molecules such as hydrogen peroxide to pass through and finally reaches the platinum electrode where it is oxidised to produce electrons.

Immobilized enzyme reaction:

$$\text{D-glucose} + O_2 \xrightarrow{\text{glucose oxidase}} \text{D-glucano-}\delta\text{-lactone} + H_2O_2 \quad (7)$$

Anode reaction:

$$H_2O_2 \xrightarrow{\text{platinum anode}} 2H^+ + O_2 + 2e^- \quad (8)$$

Each half chamber was filled with 41 ml of CCM. The donor phase also contained 8 mg/ml of glucose solution. The diffusion of glucose was monitored by withdrawing samples using a plastic syringe from both the chambers, at intervals of 1 h for a period of 8-9 h. The samples were placed in a glass cuvette and 25 µl were aspirated by the sipper for glucose concentration determination. The volume loss for each chamber remains consistent for every sample, thus the issue of keeping the volume constant can be ignored. All diffusion experiments were conducted in duplicate.

2.7. Determination of glucose diffusion coefficient in liquid

Diffusion coefficient of glucose in liquid media is an important factor to evaluate tortuosity. In this study, Stokes-Einstein equation is considered to evaluate this parameter for both water and CCM:

$$D = \frac{k_B T}{6\pi\eta r} \quad (9)$$

where k_B is Boltzmann's constant with a value of 1.3807 x 10^{-23} J/K, T is the working temperature in K, η is the liquid dynamic viscosity in kg/m/s and r is the Stokes radius of glucose with a value of 3.65 x 10-^{10} m (Bouchoux et al., 2005). The liquid dynamic viscosity is determined in-house using a U-tube viscometer (Poulten, Selfe & Lee Ltd, Essex, UK) (Kim et al., 2002), which are provided in Table 4. This gave kinematic viscosity, which were converted to dynamic viscosity. The experiments for the measurements of the fluid viscosity were performed at two operating temperatures, i.e., 27 and 37 ± 1°C for both water and CCM.

Table 4. Dynamic viscosities of liquids at different temperatures (determined in-house using a U-tube viscometer)

Liquid	**Temperature (**°C)	**Average dynamic viscosity (kg/m/s)**
Water	27 ± 1	0.000865269
	37 ± 1	0.000649516
CCM	27 ± 1	0.001306489
	37 ± 1	0.001100855

3. Results and discussions

To investigate the relationship between diffusion and membrane morphology, the microstructures of all the materials were investigated using a scanning electron microscopy (SEM) as discussed in the next section. The diffusion of glucose across membranes and scaffolds saturated in water and CCM was monitored. The results show that the diffusion coefficient is higher at a larger pore size, indicating least resistance of glucose molecules diffusing through the channel. Porosity and tortuosity were also determined to develop a correlation between diffusion and membrane morphology with porosity and tortuosity.

3.1. Material characterisation

SEM was utilized to observe the morphology of membranes and scaffolds used in this study. The dry samples were placed on a sample stand and coated with carbon. The high voltage SEM (Cambridge Stereoscan 360 SEM) was used to view the surface morphology of the investigated membranes and scaffolds. Figure 2 presents typical SEM images of PVDF membrane, CN membrane, PCL scaffold, PLLA

scaffold and collagen scaffold. The photographs show the distribution of pores and channels within the material where Figure 2a and 2b show the pore distribution of the membranes. Please note that Figures 2a and 2b have different scale bars. Figure 2c-2e show the distribution of channels and that collagen scaffold has relatively straight orientation and larger pores and this attributes to the diffusivity value presented in Table 6.

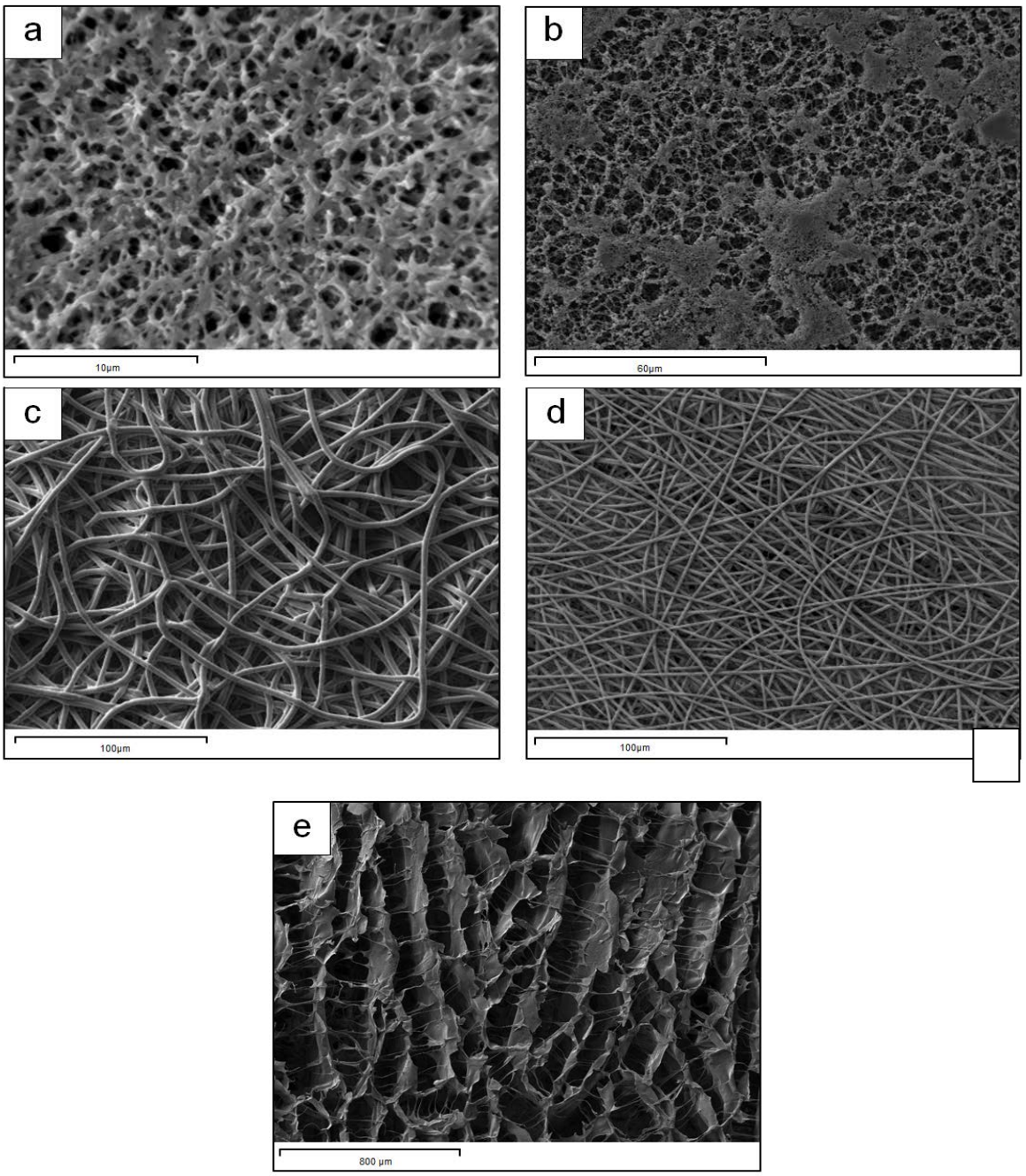

Figure 2. SEM micrographs showing surface morphology of the selected sample materials: (a) PVDF membrane, (b) Cellulose Nitrate membrane, (c) PCL scaffold, (d) PLLA scaffold and (e) Collagen scaffold

Pore size distribution across the surface of the material was also investigated (Figure 3) using the software ImageJ. It is done manually as described in section 2.4 and the procedure is reproducible. Most results are in good agreement with the manufacturer's size rating except for PVDF membrane. PVDF gave a higher mean pore size than the rating and can be ignored.

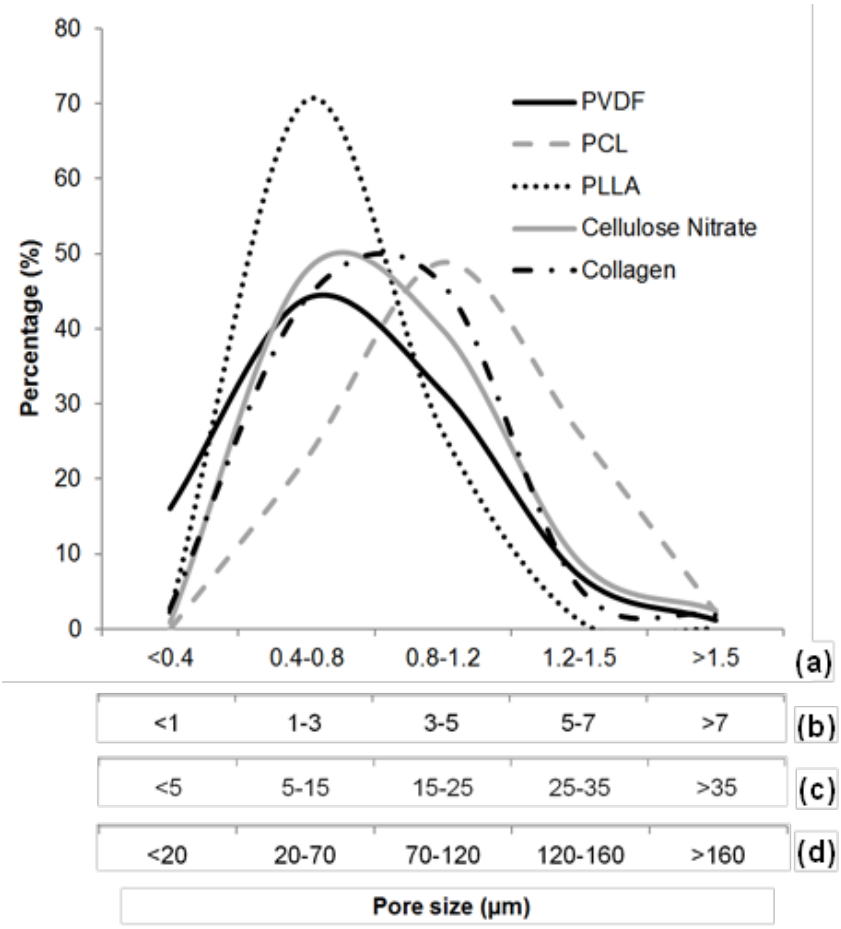

Figure 3. Average pore size distribution of membrane/scaffold as determined by us; x-axis scales are referred as follows: (a) Cellulose Nitrate membrane, (b) PVDF membrane, (c) PCL and PLLA scaffolds and (d) Collagen scaffold. The pore sizes have been manually obtained using ImageJ

3.2. Atomic force microscopy (AFM) observation for surface roughness

Atomic force microscopy is a characterisation method and presents high possibilities of application in both the field of microscopy observation and characterisation of various surfaces (Ochoa et al., 2001). The difference between AFM and SEM is that AFM can be used to determine 3D surface topography/roughness while SEM is used to determine pore size, both of which have been reported to affect the diffusion process. Figure 4 shows the 3D AFM images of cellulose nitrate (CN) membrane and PVDF membrane at a scan area of 10 µm using an atomic force microscope model Topometrix Explorer (Veeco Explorer AFM, Santa Barbara, USA) with a high resonant frequency (HRF) silicon probe and tapping mode as the imaging mode. The nodules are seen as bright high peaks.

The results for roughness parameters R_a and R_{rms} are presented in Table 5. R_a is the average surface roughness while R_{rms} is the root mean squared values. The average surface roughness values and the root mean squared values were estimated by the AFM software using the following expressions (Henke et al., 2002):

$$R_a = \frac{1}{N}\sum_{i=1}^{N}|z_i| \quad (10)$$

$$R_{rms} = \sqrt{\frac{1}{N}\sum_{i=1}^{N} z_i^2} \quad (11)$$

where N is the number of points sampled on the surface and z_i is the surface height variation of the point ($\pm z$) from the mean surface level.

A

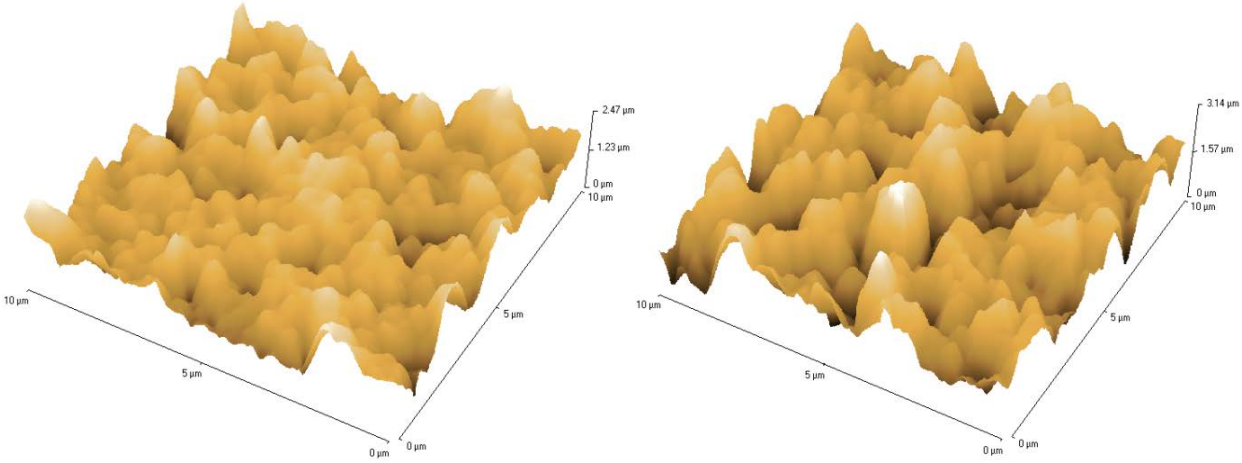

B

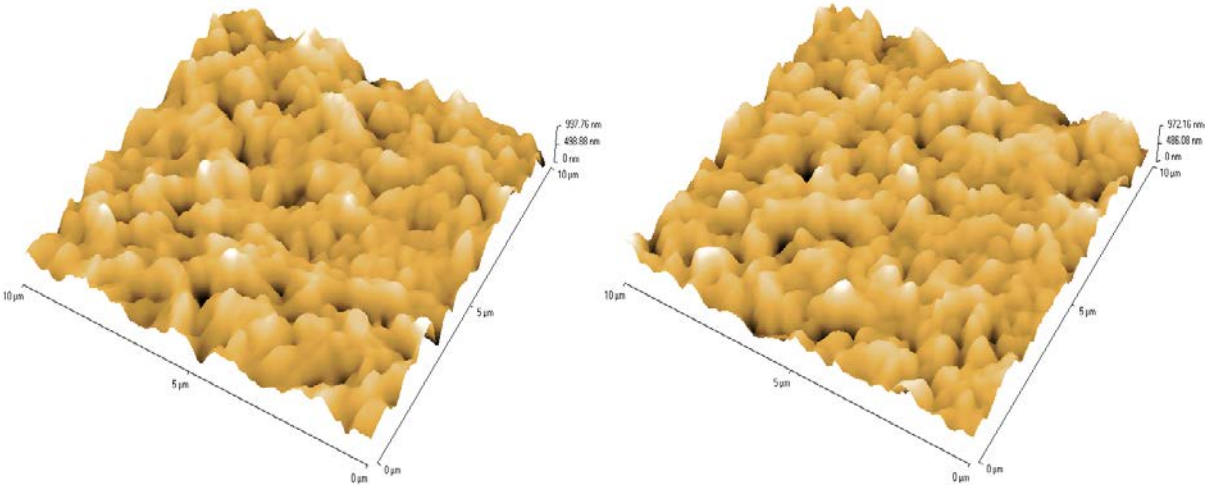

Figure 4. 3D AFM topographic images of (A) CN and (B) PVDF membranes

When the surface consists of deep depressions and high peaks, high roughness parameters are expected (Idris et al., 2007). It was also observed from other study that less tightly packed nodules

created a rough surface indicated by the high roughness parameter values (Idris et al., 2007). The change in the roughness parameters is proportional to the change in the pore size (Bessieres et al., 1996). The values in Table 5 clearly shows that PVDF membrane with a smaller pore size than cellulose nitrate membrane has lower surface roughness values and the 3D AFM image also shows that PVDF membrane has lower peaks as compared to cellulose nitrate membrane.

Comparison between Figure 4A and Figure 4B indicates that the nodules are slightly merged and much lower peaks observed. In theory, this means that the roughness parameter decreases and it agrees well with the values presented in Table 5. It has been shown in other studies (Goodyer and Bunge, 2012; Idris et al., 2007) that high surface roughness on membranes indicates increased flux as well as decreased diffusion path length. A decrease in diffusion path length may imply less tortuous pores/channels, increasing the ease of diffusion and this is reflected in the diffusion coefficient values obtained in Table 6 where cellulose nitrate membrane has a higher average diffusion coefficient value than that of PVDF membrane. The surface topography of the scaffolds is not included in this paper due to their high height ranges on small scanned areas which are built for the atomic force microscope used in this study.

Table 5. Roughness parameters of Cellulose Nitrate and Polyvinylidene Fluoride (PVDF) membranes

Membrane	R_a (nm)	R_{rms} (nm)
PVDF	164.3	208.6
	144.9	181.2
Cellulose Nitrate	286.2	367.2
	440.9	548.8

3.3. Glucose diffusion analysis

The basis for engaging different pore size and shapes tissue engineering membranes and scaffolds is to study if the varying morphological porous structures of the materials engaged have an effect on the diffusion of glucose. Typical curves for the temporal change in glucose concentration for both donor and receptor phases are shown in Figure 5. All other membranes show similar pattern as depicted in Figure 5. It can be clearly seen that this measurement gives a smooth concentration change. Table 6 summarizes the results from all these measurements. As expected, the effective diffusion coefficient is higher for a material with larger pore size. Figure 2e highlights the morphology of collagen scaffold that enables a relatively low resistance to diffusion of glucose molecules through the scaffold. The image clearly shows relatively straight channels and larger pores in comparison to other

scaffolds/membranes, thus providing less hindrance to glucose molecules diffusing through the path length. All other membranes/scaffolds' compositions are much more intertwined, thus providing more resistance to glucose diffusion through the materials (Figure 2a-2d). This is reflected in the diffusion coefficient values shown in Table 6 where PVDF membrane with the smallest pore size of 0.1 μm has the smallest glucose diffusivity while collagen scaffold with 80 μm pore size has the largest glucose diffusivity. They show that the corresponding diffusion coefficient increases with increasing pore size of the material. This is true independent of the media used. This effect can be explained with the fact that the pore radius increases. However it must be noted that apart from pore size, other microscopic properties such as porosity and tortuosity also have an effect on diffusion. It is also apparent that the results for both water and CCM saturated membranes/scaffolds are significantly different. The glucose diffusion coefficients of membranes and scaffolds saturated with CCM are significantly reduced at a given temperature. This shows that other molecules present in CCM have significant influence with respect to diffusion.

It is worth pointing out that the diffusion coefficient for the materials increases from 27°C to 37°C. This is apparent for both water and CCM saturated membranes/scaffolds. This is due to a decrease in viscosity at a higher temperature. This is also due to the increased in kinetic energy of the glucose molecules at higher temperatures and the results can be seen in Table 6. However, it must be noted that the focus of this study is not to determine the influence of the temperature on the diffusion coefficient. Hence there were only two different temperatures used in the experiments in this work.

The diffusion coefficient in free media (liquid) calculated from Stokes-Einstein's equation is comparable to what have been reported in literature, as shown in Table 7. As expected, glucose diffusion through membrane/scaffold is smaller than in the liquid which is reflected in the values shown in Table 6 except for collagen scaffolds both at 27°C and 37°C. This may be due to the homogeneous and relatively parallel pore structure as can be seen from the surface morphology of the collagen scaffold in Figure 2e. Although glucose was still able to diffuse through the membrane/scaffold, the diffusion coefficient is reduced compared to its value in free media. This may be due to several reasons. The diffusion length for glucose increases due to impermeable segments of the membrane; this is an obstruction or tortuosity effect (Westrin and Axelsson, 1991). The amount of water/CCM available for diffusion is also reduced to a fraction of the total volume due to the microstructure of the material. Hence, a much lowered value compared to the diffusivity of glucose in free media.

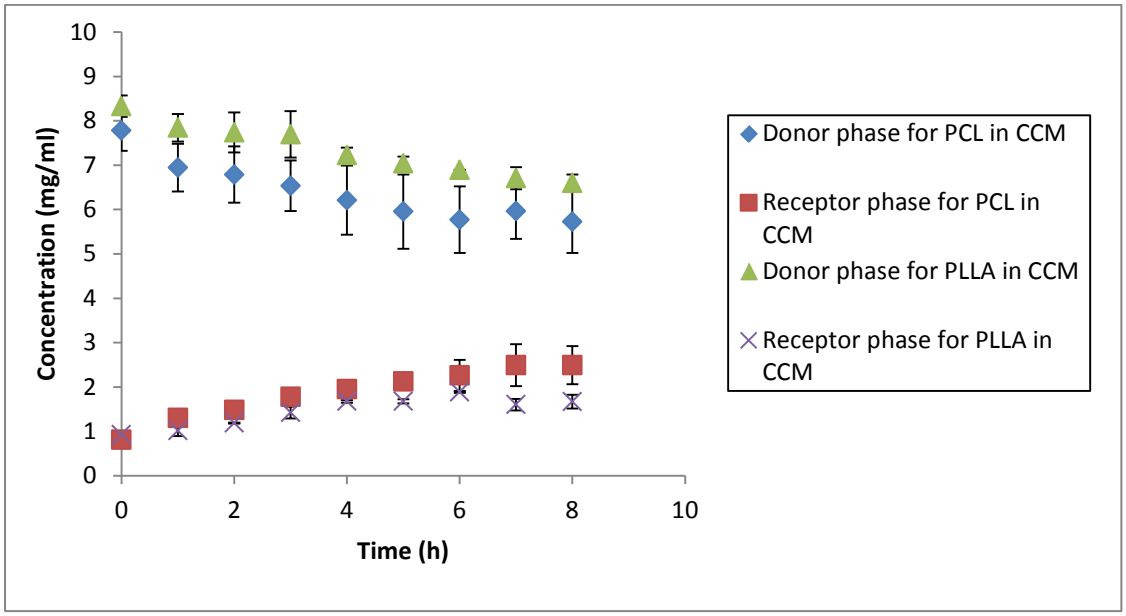

Figure 5. Diffusion cell experiment with 8 mg/ml glucose for both PCL and PLLA scaffolds saturated in CCM at 37°C

Table 6. Effective diffusion coefficients with standard deviations for glucose across membranes/scaffolds saturated in water and CCM

Material		Manufacturers' pore size (µm)	Effective diffusion coefficient (m^2/s)			
			Water at 27°C	**Water at 37°C**	**CCM at 27°C**	**CCM at 37°C**
Membrane	PVDF	0.1	$1.20 \pm 0.38 \times 10^{-10}$	$1.87 \pm 0.17 \times 10^{-10}$	$7.28 \pm 3.37 \times 10^{-11}$	$7.68 \pm 2.78 \times 10^{-11}$
	CN	0.45	$1.87 \pm 0.50 \times 10^{-10}$	$1.95 \pm 0.28 \times 10^{-10}$	$7.63 \pm 0.17 \times 10^{-11}$	$8.91 \pm 0.80 \times 10^{-11}$
Scaffold	PLLA	12-18	$2.08 \pm 0.20 \times 10^{-10}$	$2.57 \pm 0.92 \times 10^{-10}$	$1.36 \pm 0.45 \times 10^{-10}$	$1.39 \pm 0.28 \times 10^{-10}$
	PCL	20-30	$3.52 \pm 2.35 \times 10^{-10}$	$4.13 \pm 1.75 \times 10^{-10}$	$1.64 \pm 1.33 \times 10^{-10}$	$1.78 \pm 0.50 \times 10^{-10}$
	Collagen	80	$9.59 \pm 3.64 \times 10^{-9}$	$1.07 \pm 0.47 \times 10^{-8}$	$3.56 \pm 0.84 \times 10^{-9}$	$3.71 \pm 2.78 \times 10^{-9}$

393 Table 7. Comparison of the diffusion coefficient values for liquid only calculated from Stokes-Einstein's
394 equation and found in previous papers

	Calculated from Stokes-Einstein's equation (Eq. 9)	Values reported in previous papers
Diffusion coefficient in water at 27°C (m^2/s)	7.0×10^{-10}	5.4×10^{-10} (Kleinstreuer and Agarwal, 1986)
Diffusion coefficient in water at 37°C (m^2/s)	9.6×10^{-10}	9.0×10^{-10} (Buchwald, 2011)
Diffusion coefficient in CCM at 27°C (m^2/s)	4.6×10^{-10}	NA
Diffusion coefficient in CCM at 37°C (m^2/s)	5.7×10^{-10}	5.9×10^{-10} (Provin et al., 2008)

395

396 Many papers have been published on the diffusion coefficients of glucose across various membranes
397 and scaffolds at different temperatures. Papenburg et al. (2007) reported a value of 1.04×10^{-10} m^2/s
398 of glucose diffusion coefficient across PLLA scaffold saturated with water at 4°C while Shanbhag et al.
399 (2005) obtained the glucose diffusion coefficient across inverted colloidal crystal (ICC) scaffold
400 saturated in water at 25°C to be 2.7×10^{-10} m^2/s. In other studies conducted by Wang et al. (2009) and
401 Boss et al. (2012) at 37°C using hydroxypropyl chitosan (HPCTS) crosslinked with gelatin (GEL) and
402 chondroitin sulphate (CS) scaffold and asymmetric alumina membrane, both saturated in water,
403 glucose diffusion coefficient values were found to be 1.16×10^{-10} m^2/s and 1.39×10^{-10} m^2/s,
404 respectively. These reported values are within the range of experimentally-deduced diffusion
405 coefficients found in the present study (Table 6).

406 **3.4. Relationship between porosity (ϵ) and tortuosity (τ)**

407 As stated earlier, tortuous channels which are part of the pores of the membranes and scaffolds
408 hinder the diffusion of the molecules (namely, glucose in this case) through the materials. The
409 tortuosity of the molecule represents the average path length resulting from all resistances to
410 diffusion over which the molecule travels during the diffusion through the material. The fluid that
411 saturates the pores should hinder the molecular diffusion in different ways. Furthermore, as the
412 resistance to diffusion changes due to change in temperature, the tortuosity values should also
413 change.

414 The porosity is a macroscopic property of the material that represents the amount of void spaces in
415 the material and pore size distribution although in reality it may be difficult to determine the subtle
416 differences in the effects of these on the porosity values. Nevertheless, in an attempt to understand
417 how the diffusional paths of the molecules change with the pore structures of the materials, we
418 attempt to correlate the tortuosity values to porosity of the materials at different temperatures and
419 for different fluids. In traditional literature of flow and transport in porous media, many such
420 relationships can be found. Some of these relationships are reported for idealised porous material as
421 shown in Table 9. It is visible from the image (Figure 2) that PCL scaffold benefits from larger pores
422 and less tortuous channels which give a lower tortuosity value compared to other
423 membranes/scaffolds. This is depicted in Table 8 where PCL scaffold gives a tortuosity value of 2.5 and
424 consequently a higher diffusion coefficient (Table 6) in comparison to other materials. PVDF
425 membrane, with the smallest pore size, gives the largest tortuosity value of 5.1 (Table 8) and the
426 lowest diffusion coefficient value (Table 6). One can also observe from Table 8 that the tortuosities
427 vary with temperature and this is consistent with what have been found in several studies before (e.g.,
428 Gao et al., 2014; Sadighi et al., 2013; Sharma and Chellam, 2005).

429 Figure 6 shows the plot of porosity-tortuosity relations between experimental and empirical results.
430 As expected, both results are not comparable as the approaches in equation were based on a specific
431 idealised model of a porous medium (Sun et al., 2013) while the experimental results were collated
432 from different membranes and scaffolds of different pore size and microstructure.

433 Table 8. Experimentally-calculated porosity and tortuosity for all materials

Material		Manufacturers' pore size (μm)	Porosity (%)	Tortuosity (-)			
				Water at 27°C	**Water at 37°C**	**CCM at 27°C**	**CCM at 37°C**
Membrane	PVDF	0.1	69	4.0	3.5	4.4	5.1
	CN	0.45	64	2.4	3.1	3.9	4.1
Scaffold	PLLA	12-18	80	2.7	3.0	2.7	3.2
	PCL	20-30	80	1.6	1.9	2.2	2.5
	Collagen	80	72	NA	NA	NA	NA

434

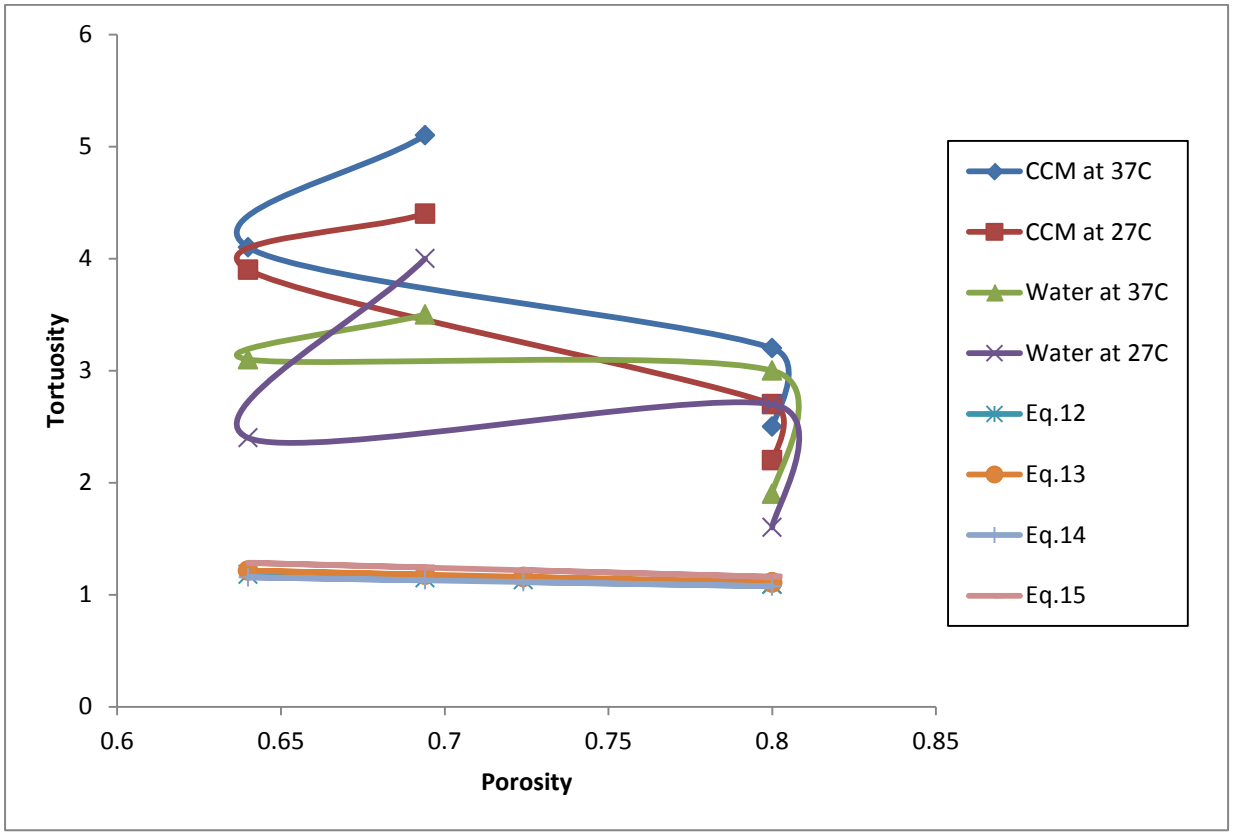

Figure 6. Comparison of porosity-tortuosity relations for all materials which are determined from the experiments in this work and four models of ideal porous material. The equations for the relationship between tortuosity and porosity for ideal porous media saturated with water (Eq. 12 – Eq. 15) are shown in Table 9.

Table 9. Porosity-tortuosity relations for ideal porous materials saturated with water

Equation number	Relation	Reference
12	$\tau = 1 - 0.41 \ln \emptyset$	Comiti and Renaud (1989)
13	$\tau = 1 - 0.49 \ln \emptyset$	Mauret and Renaud (1997); Barrande et al. (2007)
14	$\tau = 1/\emptyset^{0.33}$	Bear (1972); Dullien (1975)
15	$\tau = 1 + 0.8(1 - \emptyset)$	Koponen et al. (1996)

4. Conclusion

A diffusion cell has been constructed to measure the diffusion coefficient of glucose across varying pore size and shapes tissue engineering membranes and scaffolds which are saturated with water and CCM. The rationale behind selecting different porous structure of membranes and scaffolds in this

study was to observe how the different morphological porous structure of the materials investigated might have an effect on the glucose diffusion. The results showed the glucose diffusion coefficients for materials saturated with CCM are significantly reduced at a given temperature. This may be due to the multi-components that make up CCM and what we obtained is therefore a lumped effect from a number of inter-related phenomena. A similar trend was observed for both diffusion in water and CCM where a higher diffusion coefficient was evident with larger pores due to increased pore size. SEM enabled visual images of materials investigated including the morphology, porosity, pore size and tortuosity. Both porosity and tortuosity were evaluated in this study and based on our results, a low tortuosity value was found for the PCL scaffold used in this study and this is true independent of the media used. The low tortuosity value coupled with a higher diffusion rate compared to other materials were due to less hindrance to mass transfer and less tortuous channels. Varying the glucose concentration for diffusivity measurements and determining the mass transfer rate with the presence of biological cells (e.g., stem or epithelial cells; adherent or suspended cells) in the scaffolds will be valuable for future work.

Acknowledgment

The authors gratefully acknowledge a PhD studentship to Hazwani Suhaimi by Brunei Government which made this work possible. Department of Chemical Engineering, Loughborough University is acknowledged for its support to Shuai Wang's PhD work.

References

Abdullah NS, Das DB (2007) Modelling nutrient transport in hollow fibre membrane bioreactor for growing bone tissue with consideration of multi-component interactions, Chemical Engineering Science, Vol. 62, Issue 21, 5821-5839

Abdullah NS, Jones DR, Das DB (2009) Nutrient transport in bioreactors for bone tissue growth: Why do hollow fibre membrane bioreactors work?, Chemical Engineering Science, Vol. 64, Issue 1, 109-125

Abousleiman RI, Reyes Y, McFetridge P, Sikavitsas V (2009) Tendon tissue engineering using cell-seeded umbilical veins cultured in a mechanical stimulator, Tissue Engineering Part A, Vol. 15, Issue 4, 787-795

Andersson M, Axelsson A, Zacchi G (1997) Diffusion of glucose and insulin in a swelling N-isopropylacrylamide gel, International Journal of Pharmaceutics, Vol. 157, Issue 2, 199-208

Bai H, Liu Z, Sun DD (2012) A hierarchically structured and multifunctional membrane for water treatment, Applied Catalysis B: Environmental, Vol. 111-112, 571-577

Baptista RP, Fluri DA, Zandstra PW (2013) High density continuous production of murine pluripotent cells in an acoustic perfused bioreactor at different oxygen concentrations, Biotechnology and Bioengineering, Vol. 110, Issue 2, 648-655

Barrande M, Bouchet R, Denoyel R (2007) Tortuosity of porous particles, Analytical Chemistry, Vol. 79, Issue 23, 9115-9121

Bear J (1972) Dynamics of fluids in porous media, American Elsevier, New York

Bessieres A, Meireles A, Coratger M, Beauvillain R, Sanchez V (1996), Investigations of surface properties of polymeric membranes by near field microscopy, Journal of Membrane Science, Vol. 109, Issue 2, 271-284

Bica CID, Borsali R, Geisslet E, Rochas C (2001) Dynamics of cellulose whiskers in agarose gels 1: polarized dynamic light scattering, Macromolecules, Vol. 34, Issue 15, 5275-5279

Bock N, Riminucci A, Dionigi C, Russo A, Tampieri A, Landi E, Goranov VA, Marcacci M, Dediu V (2010) A novel route in bone tissue engineering: Magnetic biomimetic scaffolds, Acta Biomaterialia, Vol. 6, Issue 3, 786-796

Boss C, Meurville E, Sallese JM, Ryser P (2011) A viscosity-dependent affinity sensor for continuous monitoring of glucose in biological fluids, Biosensors and Bioelectronics, Vol. 30, Issue 1, 223-228

Boss C, Meurville E, Sallese JM, Ryser P (2012) Size-selective diffusion in nanoporous alumina membranes for a glucose affinity sensor, Journal of Membrane Science, Vol. 401-402, 217-221

Bouchoux A, Balmann HRD, Lutin F (2005) Nanofiltration of glucose and sodium lactate solutions variations of retention between single- and mixed-solute solutions, Journal of Membrane Science, Vol. 258, 123-132

Buchwald P (2011) A local glucose- and oxygen concentration-based insulin secretion model for pancreatic islets, Theoretical Biology and Medical Modelling, Vol. 8, Issue 20, 1-25

Burrin JM, Alberti KGMM (1990) What is blood glucose: Can it be measured?, Diabetic Medicine, Vol. 7, Issue 3, 199-206

Cai T, Li M, Neoh KG, Kang ET (2012) Preparation of stimuli responsive polycaprolactone membranes of controllable porous morphology *via* combined atom transfer radical polymerization, ring-opening polymerization and thiol-yne click chemistry, Journal of Materials Chemistry, Vol. 22, 16248-16258

505 Carrel A (1912) On the permanent life of tissues outside of the organism, The Journal of Experimental
506 Medicine, Vol. 15, Issue 5, 516-528

507 Chai Y, Mei LH, Lin DQ, Yao SJ (2004) Diffusion coefficients in intrahollow calcium alginate
508 microcapsules, Journal of Chemical & Engineering Data, Vol. 49, Issue 3, 475-478

509 Chao TC, Das DB (2015) Numerical simulation of coupled cell motion and nutrient transport in NASA's
510 rotating bioreactor, Chemical Engineering Journal, Vol. 259, 961–971

511 Chan C, Zamel N, Li X, Shen J (2012) Experimental measurement of effective diffusion coefficient of
512 gas diffusion layer/microporous layer in PEM fuel cells, Electochimica Acta, Vol. 65, 13-21

513 Chapman LAC, Waters SL, Shipley RJ, Byrne HM, Whiteley JP, Ellis MJ (2012) Modelling fluid and
514 nutrient transport to determine the influence of cell seeding on the growth of cell aggregates on a
515 permeable membrane, European Cells and Materials, Vol. 23, 99

516 Chen J, Liu T, Yuan WK, Zhao L (2013) Solubility and diffusivity of CO2 in polypropylene/micro-calcium
517 carbonate composites, The Journal of Supercritical Fluids, Vol. 77, 33-43

518 Chenu C, Roberson EB (1996) Diffusion of glucose in microbial extracellular polysaccharide as affected
519 by water potential, Soil Biology and Biochemistry, Vol. 28, Issue 7, 877-884

520 Choi YK, Park SM, Lee S, Khang DY, Choi DC, Lee CH (2013) Characterization and theoretical analysis of
521 isoporous cycloaliphatic polyurethane membrane for water treatment, Desalination and Water
522 Treatment, 1-7

523 Chu TMG, Orton DG, Hollister SJ, Feinberg SE, Halloran JW (2002) Mechanical and *in vivo* performance
524 of hydroxyapatite implants with controlled architectures, Biomaterials, Vol. 23, Issue 5, 1283-1293

525 Clarke WL, Cox D, Gonder-Frederick LA, Carter W, Pohl SL (1987) Evaluating clinical accuracy of
526 systems for self-monitoring of blood glucose, Diabetes Care, Vol. 10, 622-628

527 Cleary J, Bromberg LE, Magner E (2003) Diffusion and release of solutes in pluronic-g-poly(acrylic acid)
528 hydrogels, Langmuir, Vol. 9, Issue 22, 9162-9172

529 Comiti J, Renaud M (1989) A new model for determining mean structure parameters of fixed beds
530 from pressure drop measurements: application to beds packed with parallelepipedal particles,
531 Chemical Engineering Science, Vol. 44, Issue 7, 1539-1545

532 Crank J (1975) The Mathematics of diffusion, Oxford University Press, Oxford

533 Curcio E, De Bartolo L, Barbieri G, Rende M, Giorno L, Morelli S, Drioli E (2005) Diffusive and
534 convective transport through hollow fiber membranes for liver cell culture, Journal of Biotechnology,
535 Vol. 117, Issue 3, 309-321

536 Cussler EL (2009) Diffusion: mass transfer in fluid systems, 3rd edition, United States of America:
537 Cambridge University Press, New York

538 Das DB (2007) Multiscale simulation of nutrient transport in hollow fibre membrane bioreactor for
539 growing bone tissue: Sub-cellular scale and beyond, Chemical Engineering Science, Vol. 62, Issue 13,
540 3627-3639, doi: 10.1016/j.ces.2007.02.054

541 Deans TL, Singh A, Gibson M, Elisseeff JH (2012) Regulating synthetic gene networks in 3D materials,
542 Proceedings of the National Academy of Sciences of the United States of America, Vol. 109, Issue 38,
543 15217-15222

544 Dionne KE, Cain BM, Li RH, Bell WJ, Doherty EJ, Rein DH, Lysaght MJ, Gentile FT (1996) Transport
545 characterization of membranes for immunoisolation, Biomaterials, Vol. 17, Issue 3, 257-266

546 Dullien FAL (1975) Prediction of “tortuosity factors” from pore structure data, American Institute of
547 Chemical Engineers Journal, Vol. 21, Issue 4, 820-822

548 Ellis MJ, Chaudhuri JB (2006) Poly(lactic-co-glycolic acid) hollow fibre membranes for use as a tissue
549 engineering scaffold, Biotechnology and Bioengineering, Vol. 96, Issue 1, 177-187

550 Ellis SJ, Velayutham M, Velan SS, Petersen EF, Zweier JL, Kuppusamy P, Spencer RGS (2001) EPR
551 oxygen mapping (EPROM) of engineered cartilage grown in a hollow-fiber bioreactor, Magnetic
552 Resonance in Medicine, Vol. 46, Issue 4, 819-826

553 Felder RM, Huvard GS (1980) Methods of experimental physics, Academic Press, NY, Vol. 16, 315

554 Florczyk SJ, Wang K, Jana S, Wood DL, Sytsma SK, Sham JG, Kievit FM, Zhang M (2013) Porous
555 chitosan-hyaluronic acid scaffolds as a mimic of glioblastoma micronenvironment ECM, Biomaterials

556 Gao X, da Costa JCD, Bhatia SK (2014) Understanding the diffusional tortuosity of porous materials: an
557 effective medium theory perspective, Chemical Engineering Science, Vol. 110, 55-71

558 George KA, Wentrup-Byrne E, Hill DJT, Whittaker AK (2004) Investigation into the diffusion of water
559 into HEMA-co-MOEP hydrogels, Biomacromolecules, Vol. 5, Issue 4, 1194-1199

560 Goodyer CE, Bunge AL (2012) Mass transfer through membranes with surface roughness, Journal of
561 Membrane Science, Vol. 409-410, 127-136

562 Grayson WL, Fr hlich M, Yeager K, Bhumiratana S, Chan M, Cannizzaro C, Wan LQ, Liu XS, Guo XE,
563 Vunjak-Novakovic G (2010) Engineering anatomically shaped human bone grafts, Proceedings of the
564 National Academy of Sciences of the United States of America, Vol. 107, Issue 8, 3299-3304

565 Guaccio A, Borselli C, Oliviero O, Netti PA (2008) Oxygen consumption of chondrocytes in agarose and
566 collagen gels: a comparative analysis, Biomaterials, Vol. 29, Issue 10, 1484-1493

567 Guan S, Zhang XL, Lin XM, Liu TQ, Ma XH, Cui ZF (2013) Chitosan/gelatin porous scaffolds containing
568 hyaluronic acid and heparan sulfate for neural tissue engineering, Journal of Biomaterials Science,
569 Polymer Edition, Vol. 24, Issue 8, 999-1014

570 Gutenwik J, Nilsson B, Axelsson A (2004) Determination of protein diffusion coefficients in agarose gel
571 with a diffusion cell, Biochemical Engineering Journal, Vol. 19, Issue 1, 1-7

572 Hamburger V (1997) Wilhelm Roux: visionary with a blind spot, Journal of the History of Biology, Vol.
573 30, Issue 2, 229-238

574 Henke L, Nagy N, Krull UJ (2002) An AFM determination of the effects of surface roughness caused by
575 cleaning of fused silica and glass substrates in the process of optical biosensor preparation, Biosensors
576 and Bioelectronics, Vol. 17, Issues 6-7, 547-555

577 Idris A, Zain NM, Noordin MY (2007) Synthesis, characterization and performance of asymmetric
578 polyethersulfone (PES) ultrafiltration membranes with polyethylene glycol of different molecular
579 weights as additives, Desalination, Vol. 207, Issues 1-3, 324-339

580 Jeon G, Yang SY, Kim JK (2012) Functional nanoporous membranes for drug delivery, Journal of
581 Materials Chemistry, Vol. 22, 14814-14834

582 Kang Y, Yao Y, Yin G, Huang Z, Liao X, Xu X, Zhao G (2009) A study on the *in vitro* degradation
583 properties of poly(L-lactic acid)/β-tricalcium phosphate (PLLA/β-TCP) scaffold under dynamic loading,
584 Medical Engineering & Physics, Vol. 31, Issue 5, 589-594

585 Karageorgiou V, Kaplan D (2005) Porosity of 3D biomaterial scaffolds and osteogenesis, Biomaterials,
586 Vol. 26, Issue 27, 5474-5491

587 Karande TS, Ong JL, Agrawal CM (2004) Diffusion in musculoskeletal tissue engineering scaffolds:
588 design issues related to porosity, permeability, architecture, and nutrient mixing, Annals of Biomedical
589 Engineering, Vol. 32, Issue 12, 1728-1743

590 Kellner K, Liebsch G, Klimant I, Wolfbeis OS, Blunk T, Schulz MB, Gopferich A (2002) Determination of
591 oxygen gradients in engineered tissue using a fluorescent sensor, Biotechnology and Bioengineering,
592 Vol. 80, Issue 1, 73-83

593 Keogh MB, O'Brien FJ, Daly JS (2010) Substrate stiffness and contractile behaviour modulate the
594 functional maturation of osteoblasts on a collagen-GAG scaffold, Acta Biomaterialia, Vol. 6, Issue 11,
595 4305-4313

596 Kim JY, Lee JW, Lee SJ, Park EK, Kim SY, Cho DW (2007) Development of a bone scaffold using HA
597 nanopowder and micro-stereolithography technology, Microelectronic Engineering, Vol. 84, Issues 5-
598 8, 1762-1765

599 Kim S, Cho YI, Hogenauer WN, Kensey KR (2002) A method of isolating surface tension and yield stress
600 effects in a U-shaped scanning capillary-tube viscometer using a Casson model, Journal of Non-
601 Newtonian Fluid Mechanics, Vol. 103, Issues 2-3, 205-219

602 Kimelman-Bleich N, Seliktar D, Kallai I, Helm GA, Gazit Z, Gazit D, Pelled G (2011) The effect of ex vivo
603 dynamic loading on the osteogenic differentiation of genetically engineered mesenchymal stem cell
604 method, Journal of Tissue Engineering and Regenerative Medicine, Vol. 5, Issue 5, 384-393

605 Klein E, Holland FF, Donnaud A, Lebeouf A, Eberle K (1977) Diffusive and hydraulic permeabilities of
606 commercially available cellulosic hemodialysis films and hollow fibers, Journal of Membrane Science,
607 Vol. 2, 349-364

608 Kleinstreuer C, Agarwal SS (1986) Analysis and simulation of hollow-fiber bioreactor dynamics,
609 Biotechnology and Bioengineering, Vol. 28, Issue 8, 1233-1240

610 Koponen A, Kataja M, Timonen J (1996) Tortuous flow in porous media, Physical Review E, Vol. 54,
611 Issue 1, 406-410

612 Kwak S, Lafleur M (2003) NMR self-diffusion measurements of molecular and macromolecular species
613 in dextran solutions and gels, Macromolecules, Vol. 36, Issue 9, 3189-3195

614 Leddy HA, Awad HA, Guilak F (2004) Molecular diffusion in tissue-engineered cartilage constructs:
615 Effects of scaffold material, time, and culture conditions, Journal of Biomedical Materials Research
616 Part B: Applied Biomaterials, Vol. 70B, Issue 2, 397-406

617 L'Heureux N, Dusserre N, Marini A, Garrido S, de la Fuente L, McAllister T (2007) Technology insight:
618 the evolution of tissue-engineered vascular grafts-from research to clinical practice, Nature Clinical
619 Practice Cardiovascular Medicine, Vol. 4, 389-395

620 Li ST, Liu Y, Zhou Q, Lue RF, Song L, Dong SW, Guo P, Branko K (2013) A novel axial-stress bioreactor
621 system combined with a substance exchanger for tissue engineering of 3D constructs, Tissue
622 Engineering Part C: Methods, DOI: 10.1089/ten.tec.2013.0173

623 Lindh M, Lindgren K, Carlstrom A, Masson P (1982) Electrochemical interferences with the YSI glucose
624 analyser, Clinical Chemistry, Vol. 28, Issue 4, 726-727

625 Liu C, Abedian R, Meister R, Haasper C, Hurschler C, Krettek C, Lewinski GV, Jagodzinski M (2012)
626 Influence of perfusion and compression on the proliferation and differentiation of bone mesenchymal
627 stromal cells seeded on polyurethane scaffolds, Biomaterials, Vol. 33, Issue 4, 1052-1064

628 Liu J, Hilderink J, Groothuis TA, Otto C, van Blitterswijk CA, Boer JD (2013) Monitoring nutrient
629 transport in tissue-engineered grafts, Journal of Tissue Engineering and Regenerative Medicine, DOI:
630 10.1002/term.1654

631 Longsworth LG (1952) Diffusion measurements, at 1-degree, of aqueous solutions of amino acids,
632 peptides and sugars, Journal of the American Chemical Society, Vol. 74, Issue 16, 4155-4159

633 Longsworth LG (1953) Diffusion measurements, at 25-degrees, of aqueous solutions of amino acids,
634 peptides and sugars, Journal of the American Chemical Society, Vol. 75, Issue 22, 5705-5709

635 Lu JP, Tan FW, Tang Q, Jiang TC (2013) Novel method for indirect determination of iodine in marine
636 products by atomic fluorescence spectrometry, Chemical Research in Chinese Universities, Vol. 29,
637 Issue 1, 26-29

638 Malda J, Rouwkema J, Martens DE, le Comte EP, Kooy FK, Tramper J, van Blitterswijk CA, Riesle J
639 (2004a) Oxygen gradients in tissue-engineered PEGT/PBT cartilaginous constructs: measurement and
640 modelling, Biotechnology and Bioengineering, Vol. 86, Issue 1, 9-18

641 Malda J, Woodfield TBF, van der Vloodt F, Kooy FK, Martens DE, Tramper J, van Blitterswijk CA, Riesle J
642 (2004b) The effect of PEGT/PBT scaffold architecture on oxygen gradients in tissue engineered
643 cartilaginous constructs, Biomaterials, Vol. 25, Issue 26, 5773-5780

644 Martin AN (1993) Physical Pharmacy: physical chemical principles in the pharmaceutical sciences, Lea
645 and Febiger, Philadelphia, 337

646 Mauck RL, Hung CT, Ateshian GA (2003a) Modeling of neutral solute transport in a dynamically loaded
647 porous permeable gel: implications for articular cartilage biosynthesis and tissue engineering, Journal
648 of Biomechanical Engineering, Vol. 125, Issue 5, 602-614

649 Mauret E, Renaud M (1997) Transport phenomena in multi-particle systems-I. Limits of applicability of
650 capillary model in high voidage beds-application to fixed beds of fibers and fluidized beds of spheres,
651 Chemical Engineering Science, Vol. 52, Issue 11, 1807-1817

652 McCain KS, Schluesche P, Harris JM (2004) Poly(amidoamine) dendrimers as nanoscale diffusion
653 probes in sol-gel films investigated by total internal reflection fluorescence spectroscopy, Analytical
654 Chemistry, Vol. 76, Issue 4, 939-946

655 Meneghello G, Parker DJ, Ainsworth BJ, Perera SP, Chaudhuri JB, Ellis MJ, De Bank PA (2009)
656 Fabrication and characterization of poly(lactic-co-glycolic acid)/polyvinyl alcohol blended hollow fibre
657 membranes for tissue engineering applications, Journal of Membrane Science, Vol. 344, Issues 1-2, 55-
658 61

659 Morgan SM, Tilley S, Perera S, Ellis MJ, Kanczler J, Chaudhuri JB, Oreffo ROC (2007) Expansion of
660 human bone marrow stromal cells on poly-(DL-lactide-*co*-glycolide) (P_{DL}LGA) hollow fibres designed
661 for use in skeletal tissue engineering, Biomaterials, Vol. 28, 5332-5343

662 Napoli IED, Scaglione S, Giannoni P, Quarto R, Catapano G (2011) Mesenchymal stem cell culture in
663 convection-enhanced hollow fibre membrane bioreactors for bone tissue engineering, Journal of
664 Membrane Science, Vol. 379, Issues 1-2, 341-352

665 Napoli IED, Zanetti EM, Fragomeni G, Giuzio E, Audenino AL, Catapano G (2014) Transport modeling of
666 convection-enhanced hollow fiber membrane bioreactors for therapeutic applications, Journal of
667 Membrane Science, Vol. 471, Issue 1, 347-361

668 Nishi M, Matsumoto R, Dong J, Uemura T (2013) Engineered bone tissue associated with
669 vascularization utilizing a rotating wall vessel bioreactor, Vol. 101A, Issue 2, 421-427

670 O'Brien FJ, Harley BA, Yannas IV, Gibson LJ (2005) The effect of pore size on cell adhesion in collagen-
671 GAG scaffolds, Biomaterials, Vol. 26, Issue 4, 433-441

672 Ochoa NA, Pradanos P, Palacio L, Pagliero C, Marchese J, Hernandez A (2001) Pore size distributions
673 based on AFM imaging and retention of multidisperse polymer solutes: characterisation of
674 polyethersulfone UF membranes with dopes containing different PVP, Journal of Membrane Science,
675 Vol. 187, Issues 1-2, 227-237

676 O'Dea RD, Byrne HM, Waters SL (2013) Continuum modelling of *in vitro* tissue engineering: a review,
677 Computational Modeling in Tissue Engineering Studies in Mechanobiology, Tissue Engineering and
678 Biomaterials, Vol. 10, 229-266

679 Omae H, Sun YL, An KN, Amadio PC, Zhao C (2012) Engineered tendon with decellularized xenotendon
680 slices and bone marrow stromal cells: an *in vivo* animal study, Journal of Tissue Engineering and
681 Regenerative Medicine, Vol. 6, Issue 3, 238-244

682 Ouyang L, Randaccio L, Rulis P, Kurmaev EZ, Moewes A, Ching WY (2003) Electronic structure and
683 bonding in vitamin B_{12}, cyanocobalamin, Journal of Molecular Structure: THEOCHEM, Vol. 622, Issue 3,
684 221-227

685 Page H, Flood P, Reynaud EG (2013) Three-dimensional tissue cultures: current trends and beyond,
686 Cell and Tissue Research, Vol. 352, Issue 1, 123-131

687 Palacio L, Pradanos P, Calvo JI, Hernandez A (1999) Porosity measurements by a gas penetration
688 method and other techniques applied to membrane characterization, Thin Solid Films, Vol. 348, Issues
689 1-2, 22-29

690 Papenburg BJ, Vogelaar L, Bolhuis-Versteeg LAM, Lammertink RGH, Stamatialis D, Wessling M (2007)
691 One-step fabrication of porous micropatterned scaffolds to control cell behavior, Biomaterials, Vol. 28,
692 Issue 11, 1998-2009

693 Parizek M, Douglas TEL, Novotna K, Kromka A, Brady MA, Renzing A, Voss E, Jarosova M, Palatinus L,
694 Tesarek P, Ryparova P, Lisa V, Santos AMD, Bacakova L (2012) Nanofibrous poly(lactide-co-glycolide)
695 membranes loaded with diamond nanoparticles as promising substrates for bone tissue engineering,
696 International Journal of Nanomedicine, Vol. 7, 1931-1951

697 Paulose M, Peng L, Popat KC, Varghese OK, LaTempa TJ, Bao N, Desai TA, Grimes CA (2008) Fabrication
698 of mechanically robust, large area, polycrystalline nanotubular/porous TiO_2 membranes, Journal of
699 Membrane Science, Vol. 319, Issues 1-2, 199-205

700 Peppas NA, Wright SL (1996) Solute diffusion in poly (vinyl alcohol)/poly (acrylic acid) interpenetrating
701 networks, Macromolecules, Vol. 29, Issue 27, 8798-8804

702 Peter M, Ganesh N, Selvamurugan N, Nair SV, Furuike T, Tamura H, Jayakumar R (2010) Preparation
703 and characterization of chitosan-gelatin/nanohydroxyapatite composite scaffolds for tissue
704 engineering applications, Carbohydrate Polymers, Vol. 80, Issue 3, 687-694

705 Phanthong C, Somasundrum M (2003) The steady state current at a microdisk biosensor, Journal of
706 Electroanalytical Chemistry, Vol. 558, 1-8.

707 Pluen A, Netti PA, Jain RK, Berk DA (1999) Diffusion of macromolecules in agarose gels: comparison of
708 linear and globular configurations, Biophysical Journal, Vol. 77, Issue 1, 542-552Provin C, Takano K,

709 Sakai Y, Fujii T, Shirakashi R (2008) A method for the design of 3D scaffolds for high-density cell
710 attachment and determination of optimum perfusion culture conditions, Journal of Biomechanics, Vol.
711 41, Issue 7, 1436-1449

712 Sadighi S, Bahmani M, Mohadecy SRS (2013) Effect of pore size distribution and temperature on the
713 catalyst tortuosity, Chemical Engineering Research Bulletin, Vol. 16, 61-72

714 Sahlin JJ, Peppas NA (1996) Investigation of polymer diffusion in hydrogel laminates using near-field
715 FTIR microscopy, Macromolecules, Vol. 29, Issue 22, 7124-7129

716 Sequeira SJ, Soscia DA, Oztan B, Mosier AP, Jean-Gilles R, Gadre A, Cady NC, Yener B, Castracane J,
717 Larsen M (2012) The regulation of focal adhesion complex formation and salivary gland epithelial cell
718 organization by nanofibrous PLGA scaffolds, Biomaterials, Vol. 33, Issue 11, 3175-3186

719 Shanbhag S, Lee JW, Kotov N (2005) Diffusion in three-dimensionally ordered scaffolds with inverted
720 colloidal crystal geometry, Biomaterials, Vol. 26, Issue 27, 5581-5585

721 Sharma RR, Chellam S (2005) Temperature effects on the morphology of porous thin film composite
722 nanofiltration membranes, Environmental Science & Technology, Vol. 39, Issue 13, 5022-5030

723 Shaw M, Schy A (1981) Diffusion coefficient measurement by the 'stop-flow' method in a 5% collagen
724 gel, Biophysical Journal, Vol. 34, Issue 3, 375-381

725 Stamatialis DF, Papenburg BJ, Girones M, Saiful S, Bettahalli SNM, Schmitmeier S, Wessling M (2008)
726 Medical applications of membranes: drug delivery, artificial organs and tissue engineering, Journal of
727 Membrane Science, Vol. 308, Issues 1-2, 1-34

728 Sun Z, Tang X, Cheng G (2013) Numerical simulation for tortuosity of porous media, Microporous and
729 Mesoporous Materials, Vol. 173, 37-42

730 Umecky T, Ehara K, Omori S, Kuga T, Yui K, Funazukuri T (2013) Binary diffusion coefficients of aqueous
731 phenylalanine, tyrosine isomers, and aminobutyric acids at infinitesimal concentration and
732 temperatures from (293.2 to 333.2) K, Journal of Chemical & Engineering Data, Vol. 58, 1909-1917

733 Wang N, Krishna W, Burugapalli K, Song W, Halls J, Moussy F, Zheng Y, Ma Y, Wu Z, Li K (2013).
734 Tailored fibro-porous structure of electrospun polyurethane membranes, their size-dependent
735 properties and trans-membrane glucose diffusion, Journal of Membrane Science, 427, (5). 207–217.

736 Wang S, Liu W, Han B, Yang L (2009) Study on a hydroxypropyl chitosan-gelatin based scaffold for
737 corneal stroma tissue engineering, Applied Surface Science, Vol. 255, Issue 20, 8701-8705

738 Wang Z, Ma J (2012) The role of nonsolvent in-diffusion velocity in determining polymeric membrane
739 morphology, Desalination, Vol. 286, 69-79

740 Wartella KA, Wayne JS (2009) Bioreactor for biaxial mechanical stimulation to tissue engineered
741 constructs, Journal of Biomechanical Engineering, Vol. 131, Issue 4, Article ID 044501

742 Weng LH, Liang SM, Zhang L, Zhang XM, Xu J (2005) Transport of glucose and poly(ethylene glycol)s in
743 agarose gels studied by the refractive index method, Macromolecules, Vol. 38, Issue 12, 5236-5242

744 Westrin BA, Axelsson A (1991) Diffusion in gels containing immobilized cells: a critical review,
745 Biotechnology and Bioengineering, Vol. 38, Issue 5, 439-446

746 Wu X, Li SH, Lou LM, Chen ZR (2013) The effect of the microgravity rotating culture system on the
747 chondrogenic differentiation of bone marrow mesenchymal stem cells, Molecular Biotechnology, Vol.
748 54, Issue 2, 331-336

749 Wu YS, van Vliet LJ, Frijlink HW, van der Voort Maarschalk K (2006) The determination of relative path
750 length as a measure for tortuosity in compacts using image analysis, European Journal of
751 Pharmaceutical Sciences, Vol. 28, Issue 5, 433-440

752 Xiong Z, Yan Y, Wang S, Zhang R, Zhang C (2002) Fabrication of porous scaffolds for bone tissue
753 engineering via low-temperature deposition, Scripta Materialia, Vol. 46, Issue 11, 771-776

754 Ye H, Das DB, Triffitt JT, Cui Z (2006) Modelling nutrient transport in hollow fibre membrane
755 bioreactors for growing three-dimensional bone tissue, Journal of Membrane Science, Vol. 272, Issues
756 1-2, 169-178

757 Ye X, Farinha JPS, Oh JK, Winnik MA, Wu C (2003) Polymer diffusion in PBMA latex films using a
758 polymerizable benzophenone derivative as an energy transfer acceptor, Macromolecules, Vol. 36,
759 Issue 23, 8749-8760

760 Yu HY, Liu LQ, Tang ZQ, Yan MG, Gu JS, Wei XW (2008) Surface modification of polypropylene
761 microporous membrane to improve its antifouling characteristics in an SMBR: air plasma treatment,
762 Journal of Membrane Science, Vol. 311, Issues 1-2, 216-224

763 Yui K, Yamazaki N, Funazukuri T (2013) Infinite dilution binary diffusion coefficients for compounds
764 derived from biomass in water at 0.1 MPa and temperatures from (298.2 to 353.2) K, Journal of
765 Chemical & Engineering Data, Vol. 58, 183-186

766 Zhang Q, Jiang Y, Zhang Y, Ye Z, Tan W, Lang M (2013) Effect of porosity on long-term degradation of
767 poly(ε-caprolactone) scaffolds and their cellular response, Polymer Degradation and Stability, Vol. 98,
768 Issue 1, 209-218

769 Zhang WM, Gaberman I, Ciszkowska M (2002) Diffusion and concentration of molecular probes in
770 thermoresponsive poly(N-isopropylacrylamide) hydrogels: Effect of the volume phase transition,
771 Analytical Chemistry, Vol. 74, Issue 6, 1343-1348

Appendix

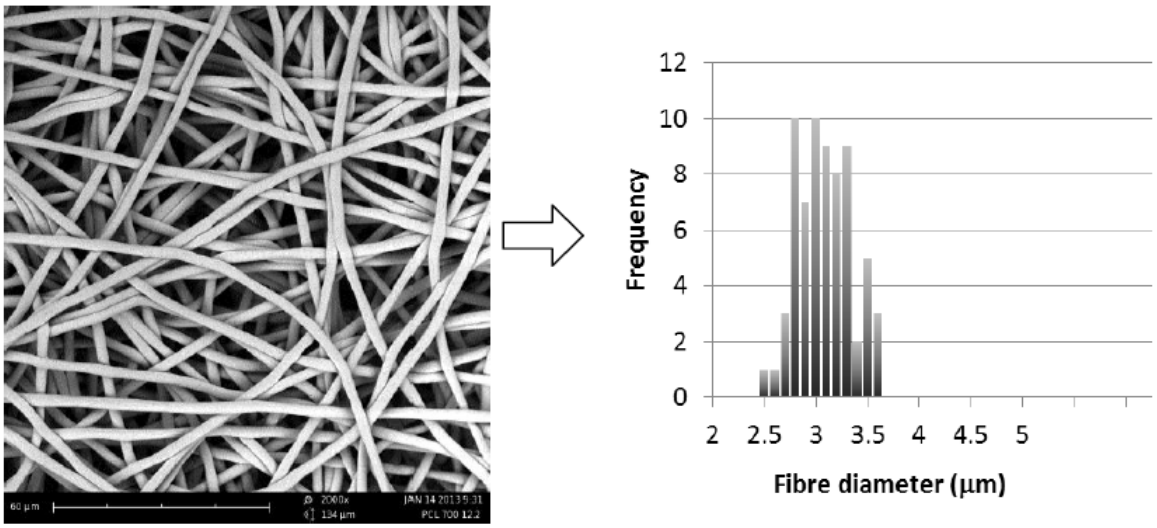

Figure A 1. SEM micrograph of PCL scaffold and its fibre diameter distribution (supplied by the manufacturer and included in the paper with their consent)

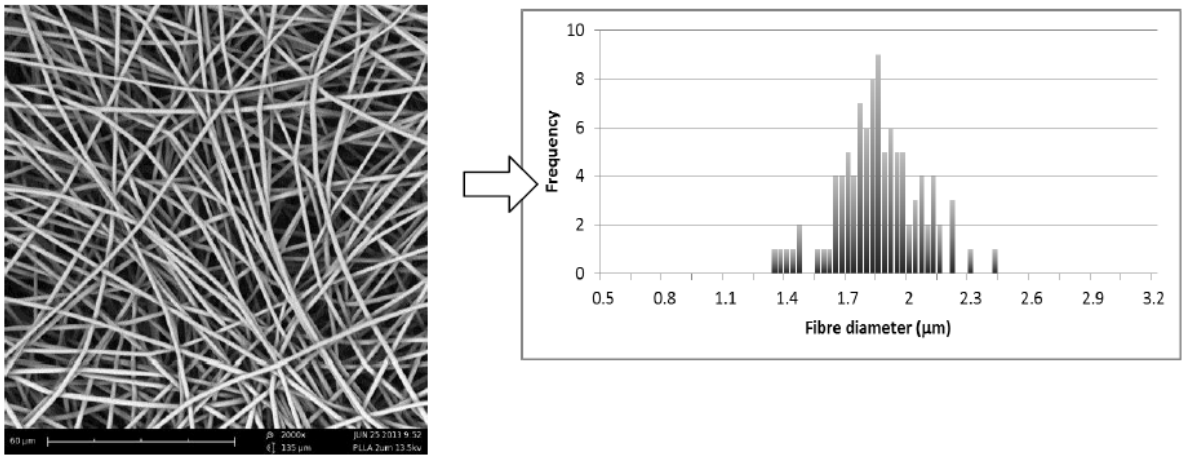

Figure A2. SEM micrograph of PLLA scaffold and its fibre diameter distribution (supplied by the manufacturer and included in the paper with their consent)